6 Supplementary Material

S1.1 Methods

Data management and naming conventions follow Zeeman et al. (2024). Steps include:

Raw CL61 ceilometers data are converted to netCDF files (L0) using raw2l1 v3.1.5b (Drouin, 2022). The widely applied STRATfinder algorithm (e.g. Molero et al., 2024; Barragán et al., 2023; Lian et al., 2023) described in Kotthaus et al. (2020a) and Kotthaus (2024a) is used with the Matlab runtime v9.3 (MathWorks Inc., 2022) to derive an aerosol-based MLH (units: m). STRATfinder uses a graph-based "pathfinder" approach (de Bruine et al., 2017) with the Dijkstra algorithm (Dijkstra, 1959). It tracks the MLH (as used here) and atmospheric boundary layer height (Kotthaus et al., 2020a). First, it calculates two-dimensional weight fields based on vertical gradients and variance indicators (Kotthaus et al., 2020a). Second, it traces layers by minimising the cost function through a time window. Third, it connects individual paths (Kotthaus et al., 2020a). The search region is constrained by user-set thresholds for characteristic heights.

Two STRATfinder versions are used: for summer *v2024.11*; (Kotthaus, 2024b), and for winter *v2025.09*. The latter has improved detection of very shallow layers (80 m) and MT is tracked more accurately (Kotthaus, 2025).

STRATfinder settings are adapted for individual cases to account for variable conditions throughout the year (Table S4). The Python (Python Software Foundation, 2025) STRATfinder QC algorithm (van Hove, 2023) is applied to flag implausible data based on empirical thresholds.

- Inputs are the reformatted raw2l1 files.
- Outputs are 1-min block-averaged MLH with 30 m vertical resolution.

Subsequent analyses use R *version 4.3.1* (R Core Team, 2023). MLH is averaged to a 15-min resolution, with time stamp indicating end of interval Some manual quality control is applied to exclude unreasonable values based on the interpretation of the backscatter profiles.

To identify the time period of the morning transition (MT) and the subsequent growth rates, we assume: (1) the morning growth can be described with a sigmoid function (2) it occurs between sunrise and time the ML reaches its peak

Note nocturnal sensible heat fluxes remain positive in urban settings (Grimmond et al., 2004; Kotthaus and Grimmond, 2014; Halios and Barlow, 2018), therefore flux cross-over time is not easily used to identify this onset.

For each morning growth period, the Levenberg-Marquardt algorithm (Moré, 1978), a non-linear least-squares regression model was used with a generalised logistic (Richards-type) function:

$$MLH(t) = A + \frac{K - A}{(1 + \nu \times e^{-B \times (t-M)})^{1/\nu}} \tag{S1}$$

where A and K are the lower and upper asymptotes, B the steepness of the curve, M the inflection point, ν a shape parameter controlling the asymmetry of the curve, and t is the predictor time. Initial parameter values are chosen using observations to improve convergence, with A and K based on MLH range:

- A = MLH_{min}
- K = $\text{MLH}_{\text{max}} \times 1.05$
- $B = 0.04$
- $\nu = 1.5$ to allow for right-skewed growth

The resulting fitted curve (Fig. S1 a) is used to calculate the derivative with respect to time to obtain instantaneous growth rates, and the normalised range ($[0, 1]$) is used to determine start of the growth period.

- MT start (MT_{start}) occurs when the normalised derivative exceeds a dimensionless empirical threshold of 0.08, indicating the onset of rapid growth.
- MT end (MT_{end}) is identified as when either the derivative passes its maximum and falls below a threshold of 0.8 or when the ML reaches its maximum height (Fig. S1 b). For days when the maximum growth occurs at the start of the MT, the 0.08 threshold is used as the end of the transition (Fig. S1 c).

Table S1: Vaisala CL61 deployment during the *urbisphere-Paris* campaign (03/2023 to 03/2024). Note the 06/2023 BOBI site moved a few hundred metre to 48.904, 2.444 (51 m agl, 97 m asl)

	CHAM	**ROIS**	**BOBI**	**HOTE**	**MEUD**	**SIRT**	**AUNA**
Lat, Lon	49.219, 2.611	49.016, 2.533	48.902, 2.452	48.855 , 2.352	48.803, 2.240	48.717, 2.208	48.431, 1.831
Placement	ground	roof	roof	ground	ground	roof	ground
Height (m agl)	0	4	3	-5	0	5	0
Height (m asl)	73	112	55	28	159	155	156
Deployment	03/2023 - 02/2024	06/2023 - 02/2024	03/2023 - 06/2023 06/2023 - 08/2023 08/2023 - 03/2024	03/2023 - 02/2024	03/2023 - 02/2024	03/2023 - 02/2024	03/2023 - 02/2024
Serial numbers	T3120614	T2920393	T2950755 U5140726 T2950755	T3250605	T3320613	T2920393 U5140726 T2950755	U4910813

Table S2: Land cover (%) Corine land cover (Copernicus Land Monitoring Service, 2019) within 10 km of each Vaisala CL61 site. Peri-urban ROIS (NE transect) has sealed surfaces and grass, whilst SIRT (SW) has more buildings. Rural site CHAM (NE) has forest and agriculture of similar proportions, whilst agriculture dominates at AUNA (SW).

	CHAM	**ROIS**	BOBI	**HOTE**	**MEUD**	**SIRT**	**AUNA**
Buildings	9.5	23.5	87.6	87.3	66.3	47.4	4.4
Sealed surfaces	0.4	24.6	6.9	5.2	2.7	2.5	0
Agriculture	43	49	0	0	1	27	91
Forest	47	1	0	0	22	18	4
Water	0	0	0	2	1	1	0
Other	0.3	1.5	4.8	5.8	7.8	4.8	0

Table S3: Eddy covariance flux tower location and deployment details.

	JUS	**SIR**	**GON**	**SAC**	**GRI**	**FON**
Lat, Lon	48.8461, 2.3548	48.713, 2.208	48.991, 2.445	48.7227, 2.142	48.8442, 1.9519	48.4763, 2.7800
Height (m agl)	0	3	51	0	0	5
Height (m asl)	73	55	97	28	159	155
Deployment	02/2023 - 12/2024	long-term	06/2022 - 12/2023	06/2023 - 02/2024	long-term	long-term
Operator	ICOS cities	SIRTA	UK Met Office	ICOS cities	ICOS	ICOS

Table S4: STRATfinder settings used (Kotthaus et al., 2020a). low lim was 80 m, except for sensor T3320613 (130 m)

Period	dayMax (m)	evening (m)	nightMax (m)	growth onset (s)
Dec-Feb	1500	700	300	10800
16 Jan	1000	500	400	10800
27 Jan	1000	500	500	18000
Sept-Nov, Mar-May	2500	1000	700	10800
Jun-Aug	4000	2500	700	10800

S1.2 Synoptic charts

Synoptic chart from UK Met Office at 12 UTC for each case study day. From www.wetter3.de/archiv_ukmet_dt.html

Table S5: Land cover (%) for 80 % source area (details given in Fig. S2) as shown in Fig. S2 - S7 for six case days characterised in Table 2 and Section 2.3).

Site	Day	Buildings	Impervious	Low vegetation	Forest	Bare soil	Water
FON	S1				100		
FON	S2				100		
FON	S3				100		
FON	W1				100		
FON	W2		1	99			
FON	W3		1	98			
GRI	S1		2	97		1	
GRI	S2			100			
GRI	S3*			94		6	
GRI	W1			100			
GRI	W2		1	93		6	
GRI	W3*			99		1	
SIR	S1	14	12	48	25		
SIR	S2	11	14	49	22	1	2
SIR	W2	16	15	25	41	0	2
SIR	W3	5	10	37	45	0	3
JUS	S1	40	30	16	12		3
JUS	S2	51	30	9	10		
JUS	S3	47	28	18	8		
JUS	W1	49	29	16	6		
GON	S1	13	24	38	24		
GON	S3	12	23	28	37		
SAC	S2	5	6	38	49	1	2
SAC	W1*	1	4	45	13	19	18
SAC	W3*	5	10	65	9	3	8

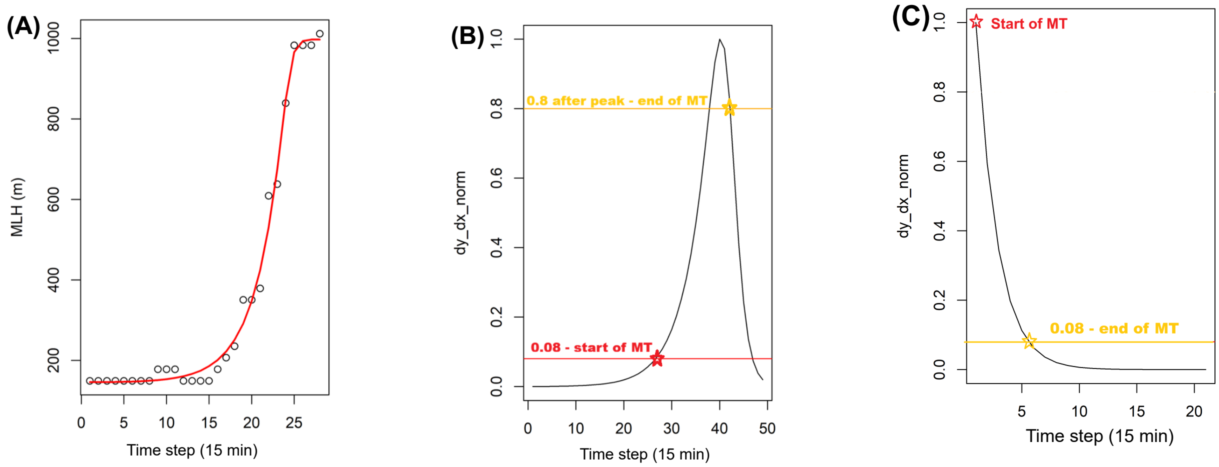

Figure S1: Curve fitting procedure to determine key mixed-layer height features (a) 15-min heights (points) with Eq. S1 fitted (line), (b) normalised derivative with thresholds (lines), plus start of morning transition (MT) (red star) and end of MT (yellow star), and (c) a case where the maximum occurs at the beginning and the end of MT (yellow) threshold is altered.

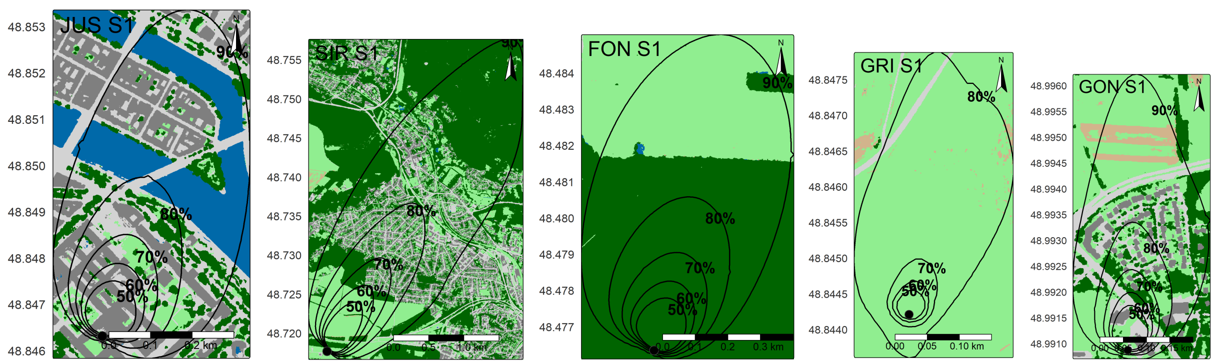

Figure S2: EC flux (Table S3) source area footprints for **S1** using Kljun et al. (2015) model. Land cover values given in S5. Key given in Fig. S5.

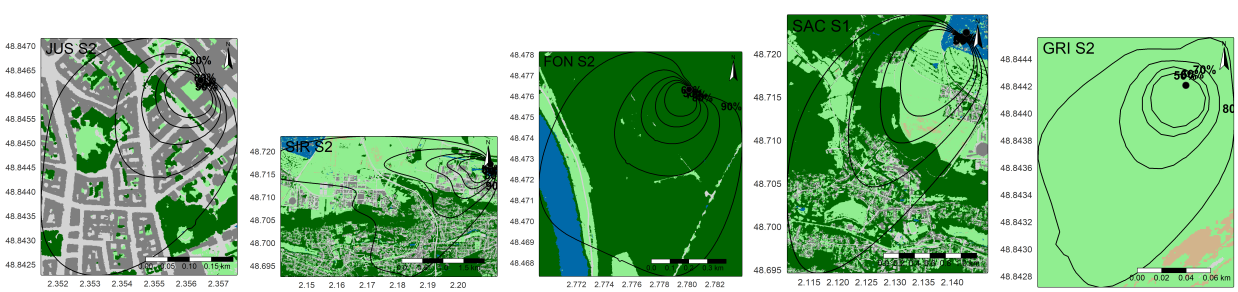

Figure S3: As Fig. S2, but for **S2**.

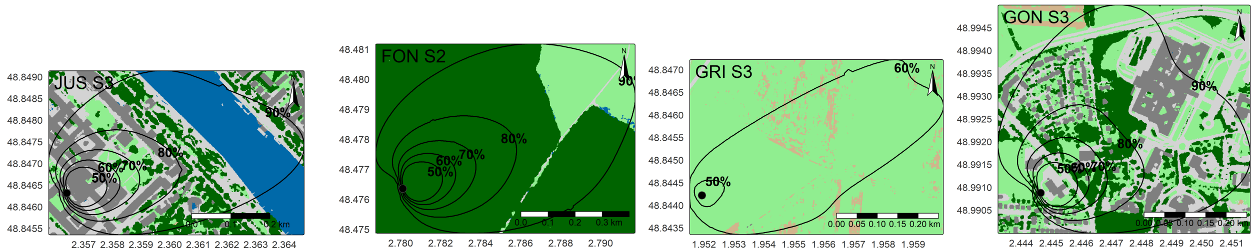

Figure S4: As Fig. S2, but for **S3**.

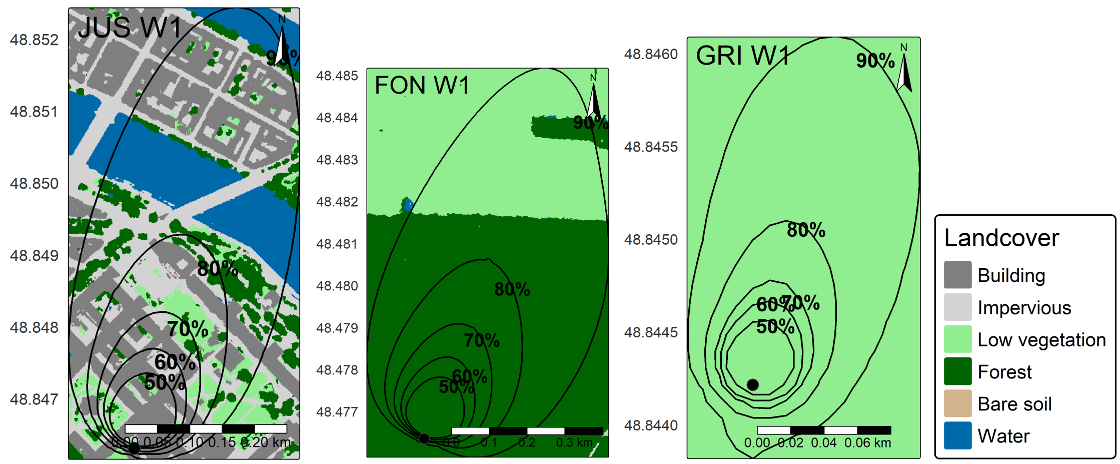

Figure S5: As Fig. S2, but for **W1**.

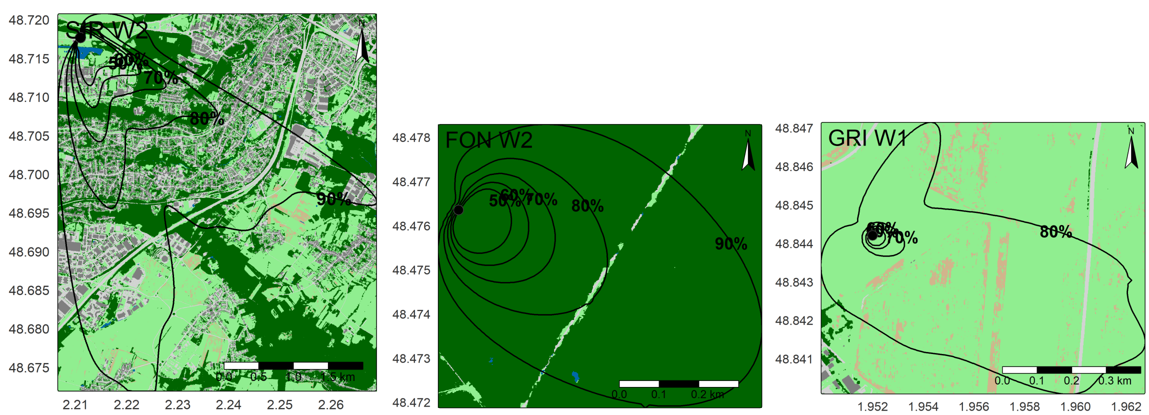

Figure S6: As Fig. S2, but for**W2**.

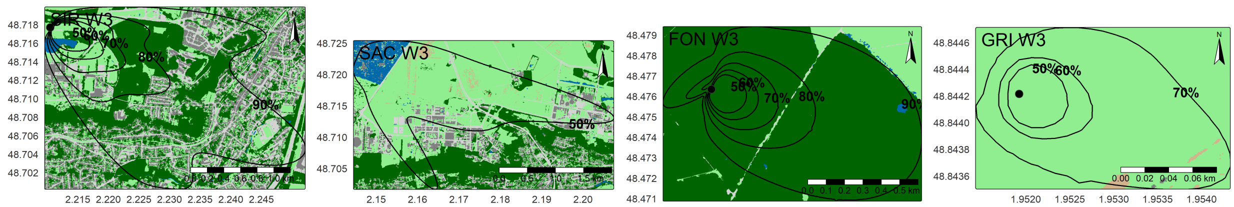

Figure S7: As Fig. S2, but for **W3**.

Table S6: Average (GR_{avg}) and maximum growth rate (GR_{max}) and maximum mixed-layer height as defined in Section 2.2.1)

Date	**CHAM** rural	**ROIS** urban fringe	**BOBI** outer city	**HOTE** inner city	**MEUD** outer city	**SIRT** urban fringe	**AUNA** rural
			Growth rate ($m\ h^{-1}$)				
across (SE)	*rural*	*urban fringe*	*outer city*	*inner city*	*outer city*	*urban fringe*	*rural*
2023-05-03	198		181	169	166	169	173
2024-01-27	345	197	201	172	81	22	132
along (NE)	*upwind*	*upwind*	*upwind*	*city*	*downwind*	*downwind*	*downwind*
2023-06-05	287		293	368	344	531	410
2024-01-11	42	74	153	45	65	73	77
along (SW)	*downwind*	*downwind*	*downwind*	*inner city*	*upwind*	*upwind*	*upwind*
2023-07-10	212	248	224	291	200	242	218
2024-01-16	345	411	307	345		437	126
			Maximum growth rate (GR_{max}) ($m\ h^{-1}$)				
across (SE)	*rural*	*urban fringe*	*city*	*inner city*	*city*	*urban fringe*	*rural*
2023-05-03	236		270	240	237	306	282
2024-01-27	392	233	295	387	134	36	175
along (NE)	*upwind*	*upwind*	*upwind*	*inner city*	*downwind*	*downwind*	*downwind*
2023-06-05	559		505	663	446	1257	785
2024-01-11	78	165	163	73	87	94	93
along (SW)	*downwind*	*downwind*	*downwind*	*inner city*	*upwind*	*upwind*	*upwind*
2023-07-10	296	265	230	332	321	286	202
2024-01-16	798	678	696	769		1033	208
			Maximum mixed-layer height (m)				
across (SE)	*rural*	*urban fringe*	*outer city*	*inner city*	*outer city*	*urban fringe*	*rural*
2023-05-03	1276		1437	1449	1403	1239	1249
2024-01-27	443	418	523	529	442	390	357
along (NE)	*upwind*	*upwind*	*upwind*	*inner city*	*downwind*	*downwind*	*downwind*
2023-06-05	1966		2256	2325	2292	2245	2270
2024-01-11	443	447	609	615	614	563	544
along (SW)	*downwind*	*downwind*	*downwind*	*inner city*	*upwind*	*upwind*	*upwind*
2023-07-10	1750	1626	1729	1693	1546	1542	1479
2024-01-16	931	993	983	1046	872	792	630

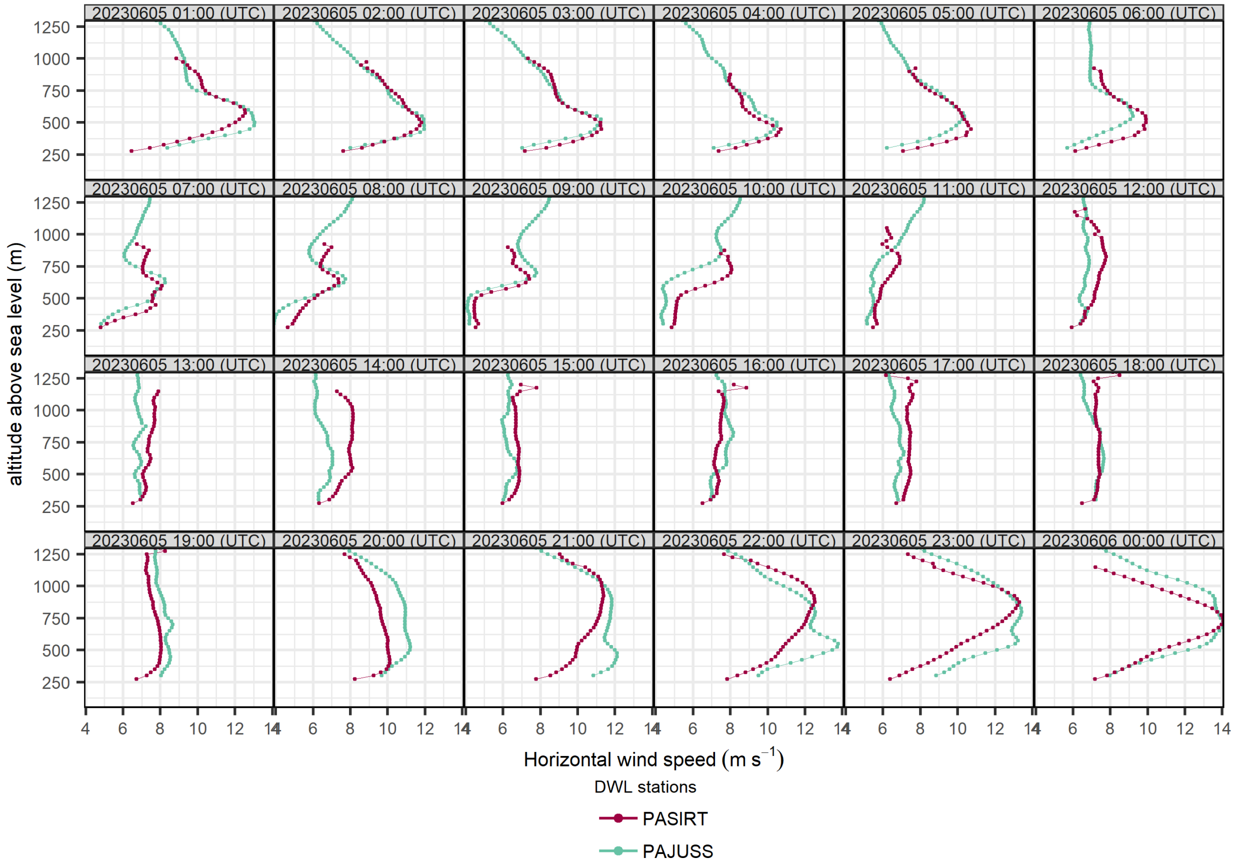

Figure S8: Nocturnal low level jet seen in Doppler wind lidar derived wind speed on **S1** (Section 3.1). Source: Morrison et al. (2025c)

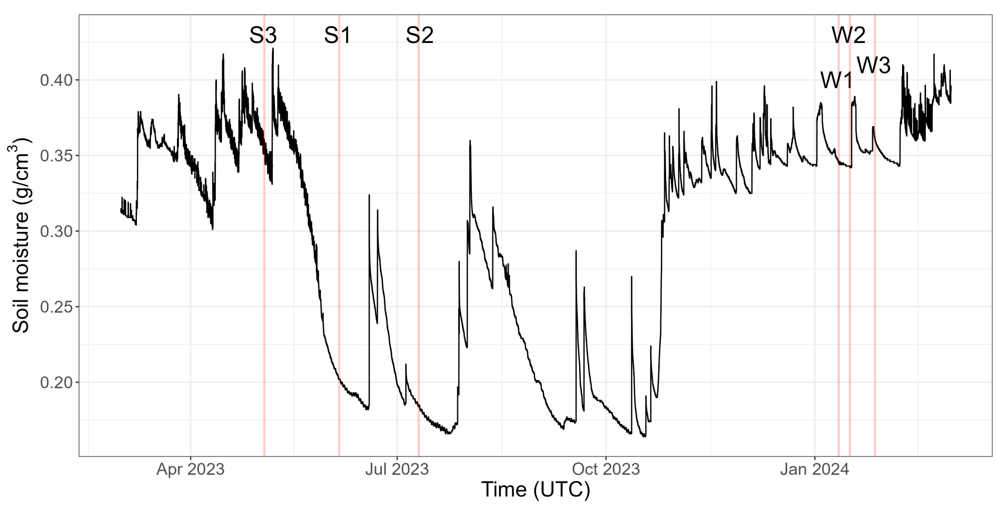

Figure S9: Soil moisture at SIRTA Observatory at 0.10 m depth.

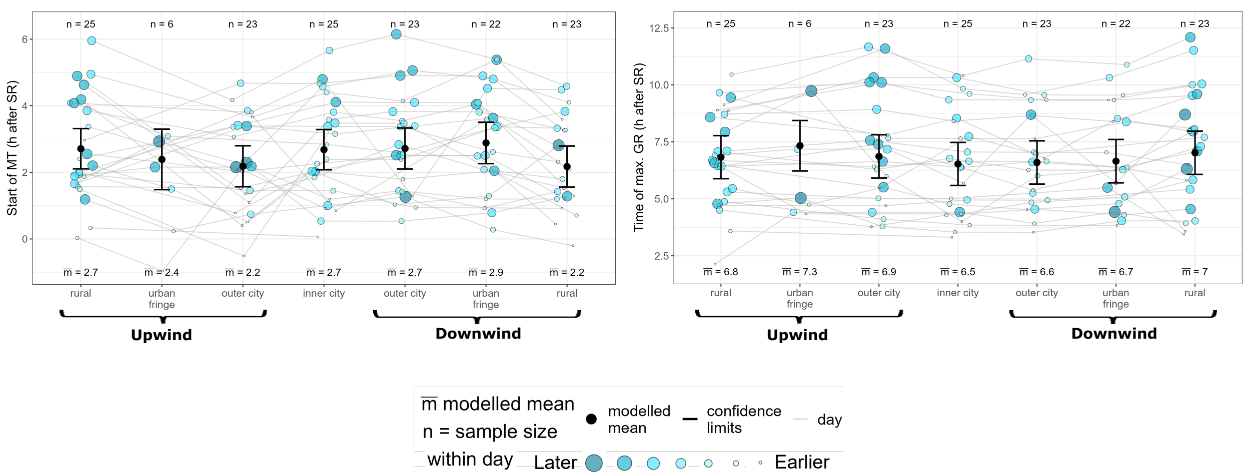

Figure S10: (a) Start of morning transition (MT) and (b) Timing of maximum growth relative to sunrise (SR), with days linked by lines and relative time (symbol size). $\overline{m}$ is modelled mean and n is number of days.